Capillarity Vol. 8, No. 2, p. 23-33, 2023

Original article

Molecular insights into structural and dynamic properties of water molecules in calcium silicate hydrate nanopores: The roles of pore size and temperature

Shaoyan Liu[1,2], Hubao A[1,2]*, Shengwen Tang[1,2], Ming-feng Kai[3], Zhibing Yang[1,2]*

[1] *State Key Laboratory of Water Resources Engineering and Management, Wuhan University, Wuhan 430072, P. R. China*
[2] *Key Laboratory of Rock Mechanics in Hydraulic Structural Engineering of the Ministry of Education, Wuhan University, Wuhan 430072, P. R. China*
[3] *Department of Civil and Environmental Engineering, The Hong Kong Polytechnic University, Hong Kong 100872, P. R. China*

Keywords:
Calcium silicate hydrate
water molecule
structural property
dynamic property
pore size
temperature

Cited as:
Liu, S., A, H., Tang, S., Kai, M., Yang, Z. Molecular insights into structural and dynamic properties of water molecules in Calcium silicate hydrate nanopores: The roles of pore size and temperature. Capillarity, 2023, 8(2): 23-33.
https://doi.org/10.46690/capi.2023.08.01

Abstract:
Calcium silicate hydrate is the primary hydration product of Portland cement and plays a crucial role in determining the strength of cement-based materials. The structural and dynamic properties of water molecules within calcium silicate hydrate nanopores have significant implications for the mechanical and durability performance of these materials. However, the influences of pore size and temperature on the properties of water molecules have not been fully explored. In this work, using molecular dynamics simulations and theoretical analysis, the evolution and mechanisms of the structural and dynamic properties of water molecules in different scenarios with various pore sizes and temperatures are systematically investigated. It is shown that the diffusion coefficients of water molecules increase with both pore size and temperature. Moreover, water molecules have a tendency to adsorb onto calcium silicate hydrate substrates, forming a distinct layered structure. As a result, the water molecules near the surfaces of calcium silicate hydrate substrates exhibit limited mobility, leading to smaller diffusion coefficients compared to those in other regions. Additionally, the distinctions in properties between water molecules and Ca^{2+} ions are elucidated and the underlying mechanisms behind these differences are also unveiled. The results and findings in this work deepen the understanding of structural and dynamic properties of water molecules within calcium silicate hydrate nanopores, providing valuable insights for improving the mechanical and durability performance of cement-based materials.

---

1. Introduction

Portland cement, as one of the most crucial building materials, has extensive applications in various structures such as roads, bridges, hydraulic and marine constructions (Heinz and Heinz, 2021; Ioannidou et al., 2022). The primary hydration product of Portland cement is calcium silicate hydrate (commonly abbreviated as calcium silicate hydrate (C-S-H)), which constitutes approximately 60%∼70% of the total hydration products in fully hydrated cement paste and is considered the main contributor to strength of cement-based materials (Dolado et al., 2007; Scrivener et al., 2019; Kai et al., 2023). Therefore, the properties of C-S-H are closely related to the performance of cement-based materials, including their mechanical and durability characteristics (Ioannidou et al., 2016; Scrivener et al., 2019; Kai et al., 2021). C-S-H is a typical porous medium with a large number of intricate nanopores (Lange et al., 1994; Ioannidou et al., 2016), which serve as channels for the transportation of water and ions. The

---

*Corresponding author.

E-mail address: liushaoyan@whu.edu.cn (S. Liu); a_hubao@whu.edu.cn (H. A); tangsw@whu.edu.cn (S. Tang); mingfeng.kai@polyu.edu.hk (M. Kai); zbyang@whu.edu.cn (Z. Yang).

Received May 1, 2023; revised May 25, 2023; accepted June 14, 2023; available online June 19, 2023.

Yandy Scientific Press

structural and dynamic properties of water molecules in C-S-H nanopores not only significantly impact the strength, shrinkage, and creep of cement-based materials but also play a crucial role in their durability issues caused by the ingress of corrosive liquids (Alderete et al., 2019; Hall, 2019). To control the performance of cement-based materials and extend the lifespan of concrete structures, a comprehensive understanding of the structural and dynamic properties of water molecules within C-S-H nanopores is imperative.

To investigate the structural and dynamic properties of water molecules within C-S-H nanopores, numerous advanced testing techniques have been employed, including nuclear magnetic resonance spectroscopy (Rakiewicz et al., 1998; Wang et al., 1998; Greener et al., 2004), broadband dielectric spectroscopy (Cerveny et al., 2011), proton field-cycling relaxometry measurement (Korb et al., 2007), quasi-elastic neutron scattering spectroscopy (Da et al., 2016). Experimental results indicate the presence of three typical types of water molecules in C-S-H: chemically bound water, physically bound water associated with matrix surface, and capillary water that exhibits no apparent interaction with C-S-H surface (Rakiewicz et al., 1998; Wang et al., 1998; Greener et al., 2004). Moreover, the forms of water molecules are closely related to their dynamic properties and can be quantitatively distinguished by diffusion coefficients. Non-bound water, due to its lesser confinement, exhibits faster diffusion rates with diffusion coefficients on the order of 10^{-9} m^2/s, which is approximately one order of magnitude higher than the diffusion coefficients of bound water (on the order of 10^{-10} m^2/s) (Bordallo et al., 2006; Peterson et al., 2006). Despite these findings, experimental studies still face limitations. Currently, most experimental techniques can only allow for measurement of an instantaneous state of water molecules, and continuous observations are still challenging. Although X-ray computed tomography can be used to detect the in-situ migration process of water molecules within cement-based materials, the resolution is typically limited to a micrometer scale, whereas the pore sizes of C-S-H nanopores are predominantly in the nanometer range (Yang et al., 2015; Kuusela et al., 2021). As a result, though accurately describing the structural and dynamic properties of water molecules within C-S-H nanopores is crucial, it still remains a challenging task.

Molecular dynamics simulations, as a complementary method, are widely used to study nanoscale phenomena (Cui et al., 2022; Liu et al., 2022) and now are extensively employed to investigate the properties of C-S-H and its interaction with water molecules as well (Hou et al., 2017; Li et al., 2017). Considering the complexity of the C-S-H structure, researchers often use natural minerals like Tobermorite and Jennite as substitutes for C-S-H (Hou and Li, 2014a, 2014b). However, these two natural minerals differ significantly from C-S-H in terms of calcium-to-silicon ratio, density, and water content, therefore cannot fully represent C-S-H. To address this issue, Pellenq et al. (2009) proposed a realistic molecular dynamics model of C-S-H based on bottom-up atomistic simulations that align well with experimental results. Researchers have utilized metrics such as density distribution and diffusion coefficients to study the structural and dynamic properties of water molecules within C-S-H nanopores (Tang et al., 2019). It has been shown that significant changes occur in the structural and dynamic properties of water molecules as the distance from C-S-H surfaces increases (Tang et al., 2019). The arrangement of water molecules transitions from an ordered state near C-S-H surface to a disordered state in bulk liquid. Additionally, water molecules near C-S-H surface experience stronger attraction from C-S-H, resulting in smaller diffusion coefficients (Hou et al., 2015). Moreover, it was also found that water molecules in the C-S-H nanopores with larger width exhibit larger diffusion coefficients (Cao et al., 2020). However, systematic studies on the influence of pore size on water molecule properties within C-S-H nanopores are still lacking. Furthermore, temperature is another key factor influencing the structural and dynamic properties of water molecules within C-S-H nanopores (Wang et al., 2020). In practical engineering, cement-based materials are inevitably exposed to environments with extremely harsh temperatures, posing severe challenges to their durability and mechanical performance. For instance, the lowest temperatures in Russia can be below 200 K (Stepanova, 1963), while the temperature in nuclear power plants may be as high as 400 K (Khan et al., 2023), and even higher in fires (Wróblewska and Kowalski, 2020). In these extreme conditions, the performance of cement-based materials deteriorates to varying degrees. Therefore, determining the influence of temperature on the properties of water molecules within C-S-H nanopores is of significant importance.

In this work, combining molecular dynamics simulations and theoretical analysis, the influences of pore size and temperature on the structural and dynamic properties of water molecules within C-S-H nanopores are systematically investigated. By quantifying the density distribution and diffusion coefficients, layered structures and anisotropic mobility of water molecules in C-S-H nanopores are identified. How the properties of water molecules evolve with pore size and temperature is also revealed. Moreover, the structural and dynamic characteristics of Ca^{2+} ions are obtained and further compared with those of water molecules. The results and findings in this work contribute to a deeper understanding of the structural and dynamic properties of water molecules in C-S-H nanopores and have implications for enhancing the mechanical and durability performance of cement-based materials.

2. Simulation method

2.1 Model construction and nanopore generation

In this work, the C-S-H model is established following the procedures proposed by Pellenq et al. (2009). The supercell of Hamid's tobermorite 11 Å without water molecules and hydroxyl groups is taken as the initial configuration. To match the Qn distribution and Ca/Si ratio obtained from experimental observations, some SiO_2 groups are randomly deleted to destroy the intact silicate chains in tobermorite. Then, the modified configuration is relaxed at ambient conditions (300 K and 1 atm) to reach an equilibrium state. Subsequently, water molecules are allowed to be inserted in the equilibrium configuration by means of grand canonical Monte Carlo simulation

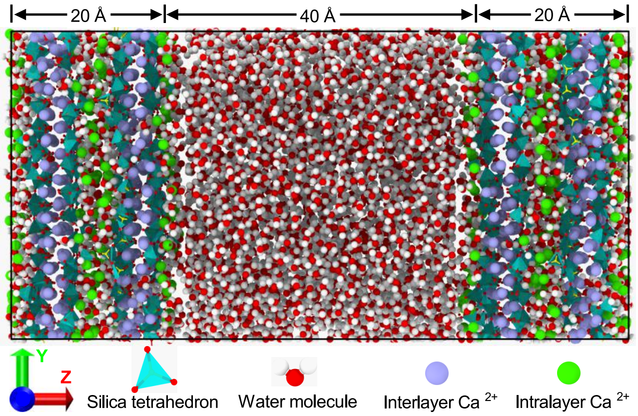

Fig. 1. Initial snapshot of the molecular dynamics simulation system utilized in this work. The case with pore size ≈ 4 nm is taken as an example.

at room temperature (300 K), during which the value of chemical potential is set to 0 eV. The water-saturated configuration is further relaxed at ambient conditions until an equilibrium state is achieved, and finally obtained configuration is treated as the C-S-H model for further simulations and analysis. Since the anisotropy of mechanical properties of C-S-H is unavoidable due to its layered structures, and the corresponding tensile strength is smallest along the direction perpendicular to layered structures of silica tetrahedral chains, i.e., Z direction in Fig. 1.

As a result, nanopores are most likely to be generated when tensile loading is applied along Z direction. Therefore, as proposed by Tang et al. (2019), we perform a uniaxial tension test on C-S-H along Z direction to generate nanopores with specified size in this work. Then, the generated nanopores are filled with water molecules, whose average density in nanopores is set to 1 $\mathrm{g/cm^3}$ (close to the density of bulk water). The finally obtained molecular dynamics simulation system is illustrated in Fig. 1.

2.2 Simulation details

Since the goal of this work is to investigate the roles of pore size and temperature on the structural and dynamic properties of water molecules in C-S-H nanopores, two groups of molecular dynamics simulations are performed. In group 1, the temperature is set to a fixed value (300 K) and remains constant, and the pore size is allowed to vary (2 nm, 4 nm, 6nm, and 8 nm). In group 2, the pore size is fixed at 4 nm, and the temperature is controlled at 100, 200, 300, and 400 K. To balance the accuracy and computational efficiency, the classical ClayFF force field is used to describe the interaction between water molecules and C-S-H (Cygan et al., 2004). All simulations are carried out on the large-scale atomic/molecular massively parallel simulator LAMMPS (Plimpton, 1995), and the temperature of simulation system is controlled by using the Nosé–Hoover method (A et al., 2023).

At the start of the simulations, C-S-H substrates are fixed, and water molecules in nanopores are relaxed for 2,000 ps to reach an equilibrium state. Then, constraints on C-S-H substrates are removed, and simulations last for another 5,000 ps. During the simulations, the time step is set to 2 fs, and the configurations of simulation system are collected every 1 ps for further analysis.

3. Results and discussion

3.1 Effects of pore size

3.1.1 Structural properties of water molecules

Density profiles along Z direction depict the distribution of water molecules, which further reflect the influence of pore size on structural properties of water molecules. Due to the existence of silica tetrahedral chains and Ca^{2+} ions, C-S-H exhibits obvious hydrophilicity (Hou et al., 2022). Thus water molecules tend to absorb on C-S-H surfaces and form layered structures as shown in Fig. 2. Density of water molecules in the central region of nanopores is visibly smaller than that in regions near C-S-H surfaces regardless of varying pore size. In addition, density of water molecules is larger in the regions closer to C-S-H surfaces, with the increase in distance from C-S-H surfaces, the influence of C-S-H on water molecules is gradually alleviated, and the corresponding density of water molecules decreases to an equilibrium value, i.e., the density of bulk water, approximately 1 $\mathrm{g/cm^3}$.

Nevertheless, the differences in structural properties of water molecules are still not negligible in nanopores of different sizes. As the interactions between water molecules in nanopores and atoms in C-S-H are closely related to the distance between them; i.e., the smaller the distance, the greater the interactions. Thus the structures of water molecules near C-S-H surfaces are much more easily to be influenced. In the nanopore with pore size of 2 nm, almost all water molecules are attracted and absorbed on C-S-H surfaces, leading to an obvious concave shape in density curve as illustrated in Fig. 2(a). With the growth of pore size, properties of water molecules in regions far away from C-S-H surfaces (i.e., central regions of C-S-H nanopres) are similar to those of bulk water, the concave density profile gradually becomes flat, especially in the central region of nanopores. In the case with relatively small pore size (2 nm as an example), there is no prominent peak on the density curve, indicating that no layered structure is formed on C-S-H surfaces. Conversely, for nanopores with larger pore sizes, there are distinct peaks on density profiles, and thus one can observe marked layering of water molecules on C-S-H surfaces.

3.1.2 Dynamic properties of water molecules and Ca^{2+} ions

In addition to structural properties, the dynamic properties of water molecules in nanopores are also significantly influenced by C-S-H surfaces. Typically, dynamic properties can be quantified by diffusion coefficients, and a smaller diffusion coefficient signifies the slower motion of atoms/molecules (Tang et al., 2019). To identify and compare the dynamic properties of water molecules comprehensively, we calculate three types of diffusion coefficients in this work, namely D (the diffusion coefficient considering movements of water molecules in all directions, see Eqs. (1)-(3)), D_{xy} (the diffusion coefficient along the direction parallel to C-S-H surfaces,

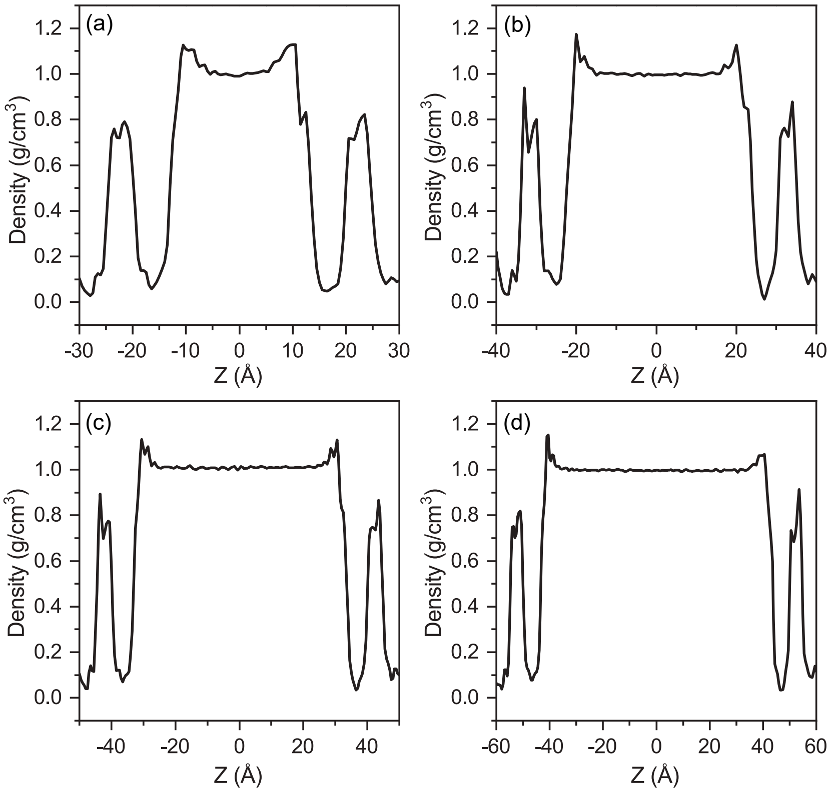

Fig. 2. Density profiles of water molecules in the cases with various pore size. (a) 2 nm, (b) 4 nm, (c) 6 nm and (d) 8 nm.

see Eqs. (4)-(5)) and D_z (the diffusion coefficient along the direction perpendicular to C-S-H surfaces, see Eqs. (6)-(7)). The calculated diffusion coefficients of water molecules in nanopores with different size is shown in Fig. 3:

$$\mathrm{MSD}_i(t) = \triangle_i^2(t) = \left\langle \left| r_i(t+\tau) - r_i(\tau) \right|^2 \right\rangle \tag{1}$$

$$\mathrm{MSD} = \frac{1}{N} \sum_{i=1}^{N} \triangle x_i^2(t) + \triangle y_i^2(t) + \triangle z_i^2(t) \tag{2}$$

$$D = \frac{1}{6} \lim_{t \to \infty} \frac{\mathrm{MSD}(t)}{t} \tag{3}$$

$$\mathrm{MSD}_{xy} = \frac{1}{N} \sum_{i=1}^{N} \triangle x_i^2(t) + \triangle y_i^2(t) \tag{4}$$

$$D_{xy} = \frac{1}{4} \lim_{t \to \infty} \frac{\mathrm{MSD}_{xy}(t)}{t} \tag{5}$$

$$MSD_z = \frac{1}{N} \sum_{i=1}^{N} \triangle z_i^2(t) \tag{6}$$

$$D_z = \frac{1}{2} \lim_{t \to \infty} \frac{MSD_z(t)}{t} \tag{7}$$

where MSD is the mean squared displacement of atoms, MSD_{xy} and MSD_z represent the parallel (XY direction) and perpendicular (Z direction) part of MSD respectively; $r_i(t+\tau)$ and $r_i(\tau)$ represent respectively the position of atom i at time $t+\tau$ and τ; τ is the time origin and its value can be set as 0, 100 fs, and so on; the bracket denotes the time averaging at multiple time origins τ. N is the total number of atoms, $\triangle x_i(t)$, $\triangle y_i(t)$ and $\triangle z_i(t)$ represent the displacement increment at time t along X, Y and Z directions, respectively.

It can be seen how pore size affects the dynamic properties of water molecules. Because of the attraction from silica-oxygen tetrahedral chains and calcium ions, water molecules tend to form high-density layered on C-S-H surfaces. Correspondingly, the movement of water molecules in the regions close to C-S-H surfaces is restricted, leading to small diffusion coefficients in all directions. As the distance between water molecules and C-S-H surfaces increases, such restriction decreases gradually and the values of diffusion coefficients (including D, D_{xy}, and D_z) grow accordingly. Therefore, it can be inferred that the diffusion coefficient of water molecules is largest in the central region of nanopores and its value increases with pore size.

The diffusion coefficients of Ca^{2+} ions are also obtained as illustrated in Fig. 4. Based on the magnitude of diffusion coefficients, Ca^{2+} ions can be roughly classified into two categories, i.e., the ones on C-S-H surfaces and others in the interior of C-S-H substrates. The movement of Ca^{2+} ions inside C-S-H substrate is seriously limited, and the corresponding diffusion coefficients are extremely small ($\approx 10^{-11}$ m^2/s). On the contrary, surface Ca^{2+} ions can move much more quickly for fewer restrictions from C-S-H substrate. Thus, the corresponding diffusion coefficients of surface Ca^{2+} ions are much larger than those of Ca^{2+} ions inside C-S-H substrate. Moreover, similar to water molecules in nanopores, the diffusion coefficients of Ca^{2+} ions increase with pore size as well.

According to Fig. 3, a phenomenon that cannot be ignored

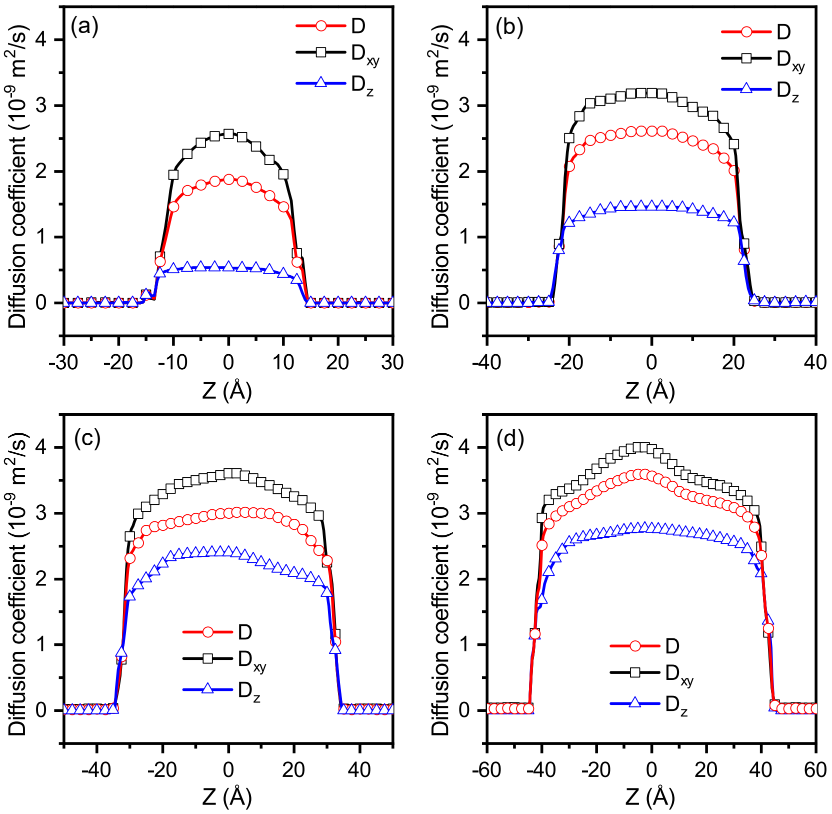

Fig. 3. Diffusion coefficient profiles of water molecules in the cases with various pore sizes. (a) 2 nm, (b) 4 nm, (c) 6 nm and (d) 8 nm.

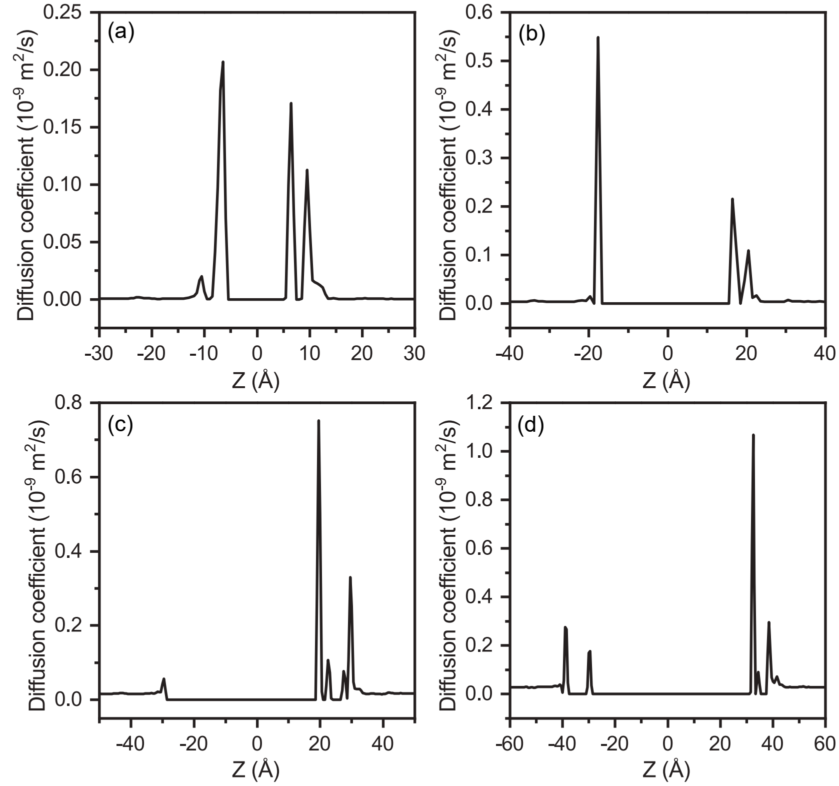

Fig. 4. Diffusion coefficient profiles of Ca^{2+} ions in the cases with various pore sizes. (a) 2 nm, (b) 4 nm, (c) 6 nm and (d) 8 nm.

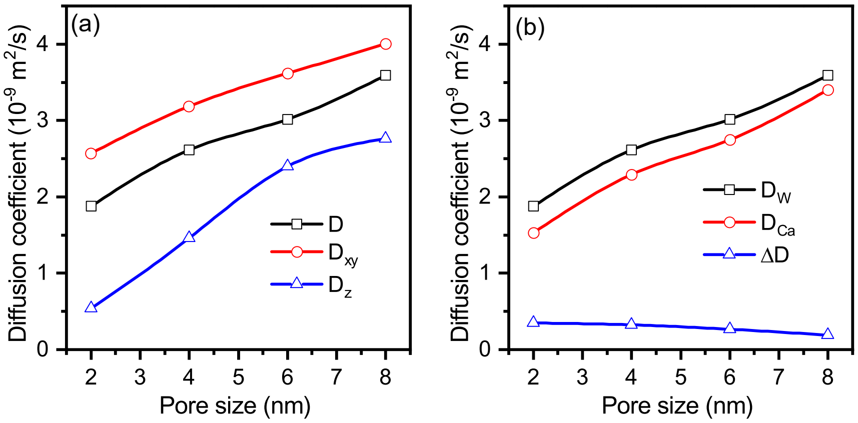

Fig. 5. (a) Relationship between overall diffusion coefficients of water molecules and sizes of nanopores, (b) comparison of overall diffusion coefficients of water molecules and Ca^{2+} ions in the nanopores of various sizes.

is the anisotropy of diffusion coefficients of water molecules in nanopores, i.e., D_z is significantly smaller than D_{xy} regardless of the varying pore size. Fig. 5(a) plots the overall diffusion coefficients of all water molecules in nanopores, it can be seen that both the values of D_{xy} and D_z increase with pore size. Moreover, although the differences between D_{xy} and D_z gradually decrease with pore size, we still see $D_z < D_{xy}$, indicating that C-S-H substrate imposes more restrictions on water molecules in Z direction. Apart from water molecules, we also obtain the diffusion coefficients of Ca^{2+} ions that escape into nanopores from C-S-H surfaces as presented in Fig. 5(b).

Consistent with the conclusions obtained from Fig. 4, diffusion coefficients of the escaped Ca^{2+} ions increase with pore size. However, Ca^{2+} ions are positively charged, which makes it possible to attract oxygen atoms in water molecules. Thus, water molecules would gather around Ca^{2+} ions and form clusters, hindering the movement of Ca^{2+} ions. As a result, the diffusion coefficients of Ca^{2+} ions are smaller than those of water molecules. Nevertheless, one should also notice that the value of $\triangle D$ (the difference between diffusion coefficient of water D_W and diffusion coefficient of Ca^{2+} ions D_{Ca}) decays with pore size.

3.2 The effect of temperature

3.2.1 Structural properties of water molecules

Fig. 6 shows the density distribution of water molecules in C-S-H nanopores with a pore size of 4 nm at a broad range of temperatures (from 100 to 400 K). Obviously, the shape of density profiles varies significantly with changing temperatures, denoting the distinct structural properties of water molecules. When temperature is extremely low (see the case with 100 K), there are numerous clearly visible fluctuations on density profile and no layered structure forms on C-S-H surfaces. Such phenomena originate from the almost imperceptible movement of water molecules caused under low temperatures, i.e., water molecules in nanopores move so slowly that they can resist the attraction of silica tetrahedral chains and Ca^{2+} ions and reside in their original positions. As temperature increases, density profiles of water molecules become smoother, and layered structures start to form on C-S-H surfaces.

However, excessive temperature hinders the formation of the layered structures of water molecules. For example, it can be seen from Figs. 3-4 that at least two distinct layers of water molecules on C-S-H surfaces at the temperature of 300 K. But when the temperature increases to 400 K, both the number of layers of water molecules and corresponding values of density decay apparently. Such phenomena are mainly caused by the following two reasons: firstly, the layered structure is related to the absorption of water molecules on C-S-H surfaces due to the existence of silica tetrahedral chains and Ca^{2+} ions after temperature increases to a certain value, water molecules would get enough kinetic energy to overcome the attractions from silica tetrahedral chains and Ca^{2+} ions. Secondly, excessive temperature induces the desorption of Ca^{2+} ions from C-S-H surfaces into nanopores (which will be discussed later), reducing the hydrophilicity of C-S-H surfaces and attraction to water molecules. As a result, when the temperature is 400 K, the layered structure of water molecules is less pronounced than that in the conditions of temperature equals 300 K.

3.2.2 Dynamic properties of water molecules and Ca^{2+} ions

Generally, the values of diffusion coefficients are directly related to the kinetic energy of water molecules, which increases with temperature, and larger kinetic energy would induce larger diffusion coefficients. Thus, diffusion coefficients increase with temperature as well as shown in Fig. 7, the diffusion coefficients of water molecules increase significantly from the magnitude of 10^{-12} m^2/s (100 K) to 10^{-9} m^2/s (400 K). Moreover, the influence of C-S-H surfaces on diffusion coefficients of water molecules cannot be ignored regardless of the increasing temperature, i.e., the diffusion coefficients of water molecules near C-S-H surfaces are smaller than those of water molecules in the middle region of nanopore. We also find D_{xy} is larger than D_z in a wide range of temperature (from 100 to 400 K), indicting the anisotropy phenomenon of diffusion coefficients.

The evolution of diffusion coefficients of Ca^{2+} ions is

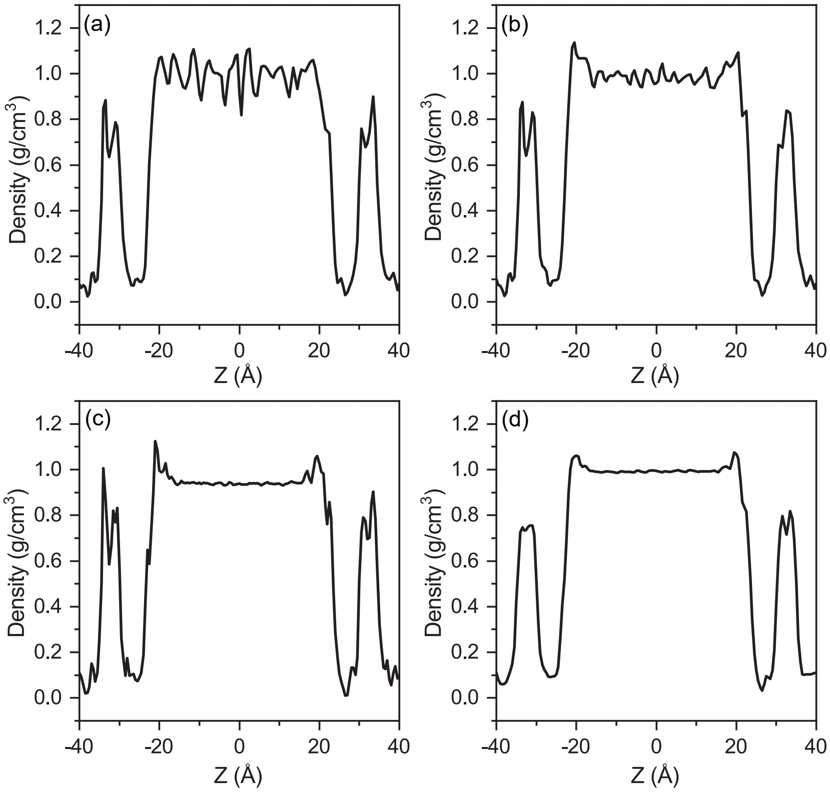

Fig. 6. Density profiles of water molecules in the cases with various temperatures. (a) 100 K, (b) 200 K, (c) 300 K and (d) 400 K.

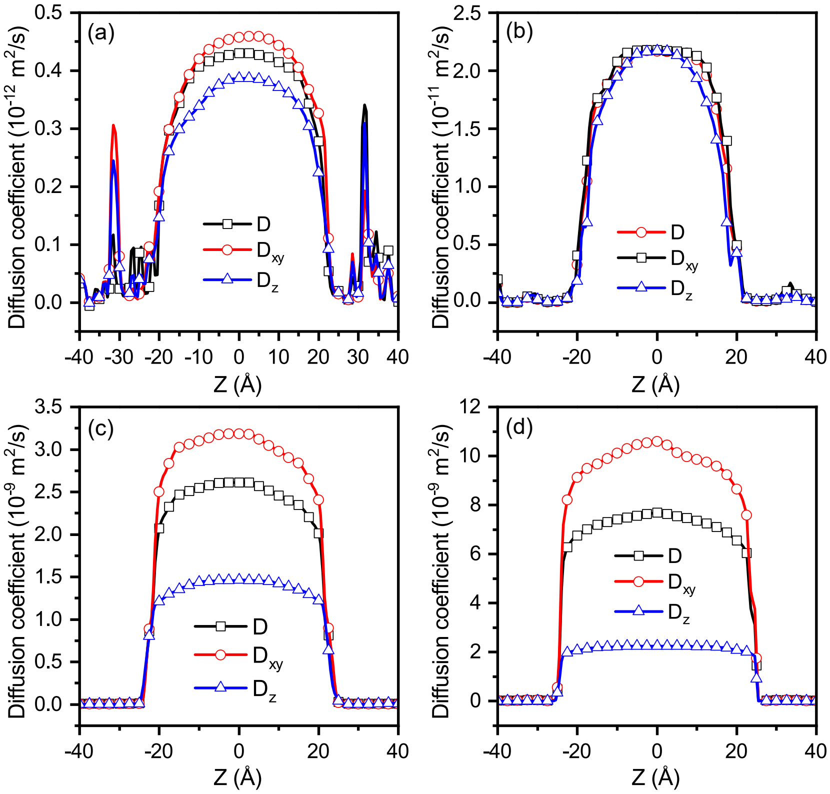

Fig. 7. Diffusion coefficient profiles of water molecules in the cases with various temperatures. (a) 100 K, (b) 200 K, (c) 300 K and (d) 400 K.

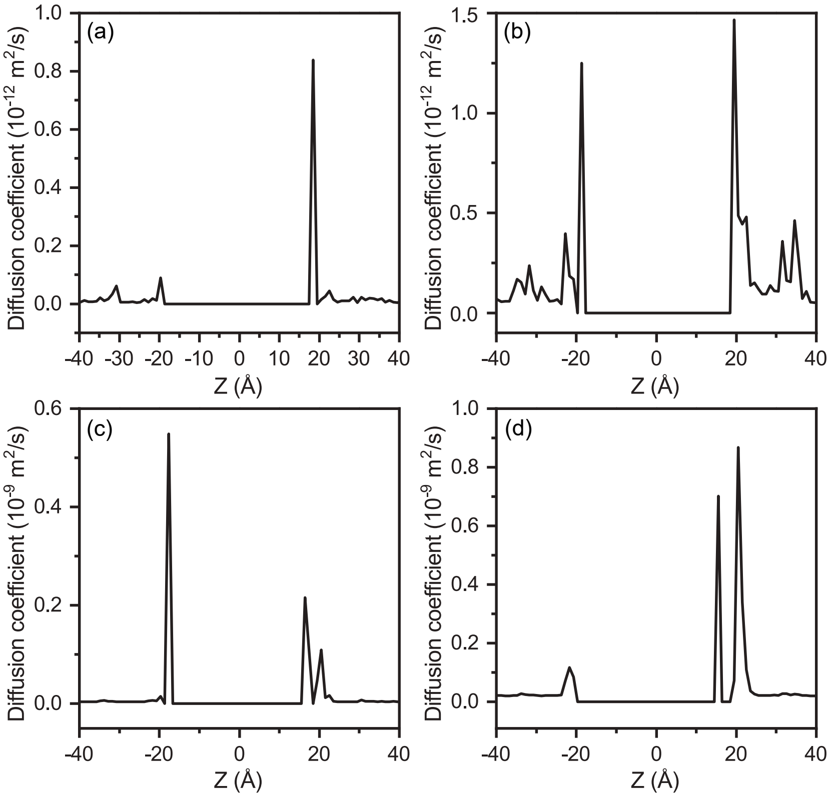

Fig. 8. Diffusion coefficient profiles of Ca^{2+} ions in the cases with various temperatures. (a) 100 K, (b) 200 K, (c) 300 K and (d) 400 K.

similar to that of water molecules, increasing significantly with temperature (see Fig. 8). When the temperature goes down to 100 K, the magnitude of diffusion coefficients is only 10^{-12} m^2/s. As temperature grows, the magnitude of diffusion coefficients increases to 10^{-12} m^2/s (at 200 K) and to 10^{-12} m^2/s (at 300∼400 K). Meanwhile, the diffusion coefficients of Ca^{2+} ions on C-S-H surfaces are significantly larger than those inside the C-S-H substrate, which is much more visible in the cases with higher temperatures.

Another noticeable phenomenon is the desorption of Ca^{2+} ions from C-S-H surfaces and moving into liquid water in nanopores due to the effect of high temperature and attraction of water molecules. Fig. 9 shows the instantaneous distribution profiles of Ca^{2+} ions at different moments in the first 500 ps simulations with various temperatures. As the simulations proceed, the desorption of Ca^{2+} ions is more obvious in the cases with higher temperature (i.e., 300 and 400 K), indicating more Ca^{2+} ions desorbed from C-S-H surfaces. Hence, there are more fluctuations (see the profiles marked with the red circle in Fig. 9) on distribution profiles. On the contrary, distribution curves of Ca^{2+} ions at different moments are almost identical when the temperature is 100 or 200 K, and no Ca^{2+} ions escape from C-S-H surfaces.

As shown in Fig. 10(a), we further examine the anisotropy of diffusion coefficients of water molecules in nanopores at different temperatures. Although both the values of D_{xy} and D_z increase with temperature, D_{xy} is always larger than D_z and the gap between them increases with temperature as well, i.e., the anisotropy phenomenon is more pronounced. Moreover, the overall diffusion coefficients of water molecules and Ca^{2+} ions in nanopores are compared in Fig. 10(b). Similar to water molecules, the diffusion coefficient of desorbed Ca^{2+} ions also increases significantly with temperature. But the movement of Ca^{2+} ions is still slower then water molecules, for water molecules tend to cluster around Ca^{2+} ions, weakening the moving capability of Ca^{2+} ions in nanopores. This phenomenon is also more pronounced when the temperature is higher, and correspondingly, the value of $\triangle D$ (the difference between the diffusion coefficients of water D_W and Ca^{2+} ions D_{Ca}) increases with temperature.

4. Conclusion

In this work, with the combined efforts of molecular dynamics simulations and theoretical analysis, the roles of pore size and temperature on structural and dynamic properties of water molecules in C-S-H nanopores are compressively investigated, in which two critical indicators, i.e., density profiles and diffusion coefficients are quantified and compared. Due to the existence of silica tetrahedral chains and Ca^{2+} ions, C-S-H surfaces exhibit obvious hydrophilicity. Thus, water molecules would be absorbed on C-S-H surfaces and form layered structures, which can be identified through density distribution profiles. When pore size is relatively small (2 nm as an example), most water molecules are attracted and absorbed on C-S-H surfaces, so there is an obvious concave shape in the density profiles. As pore size increases, there

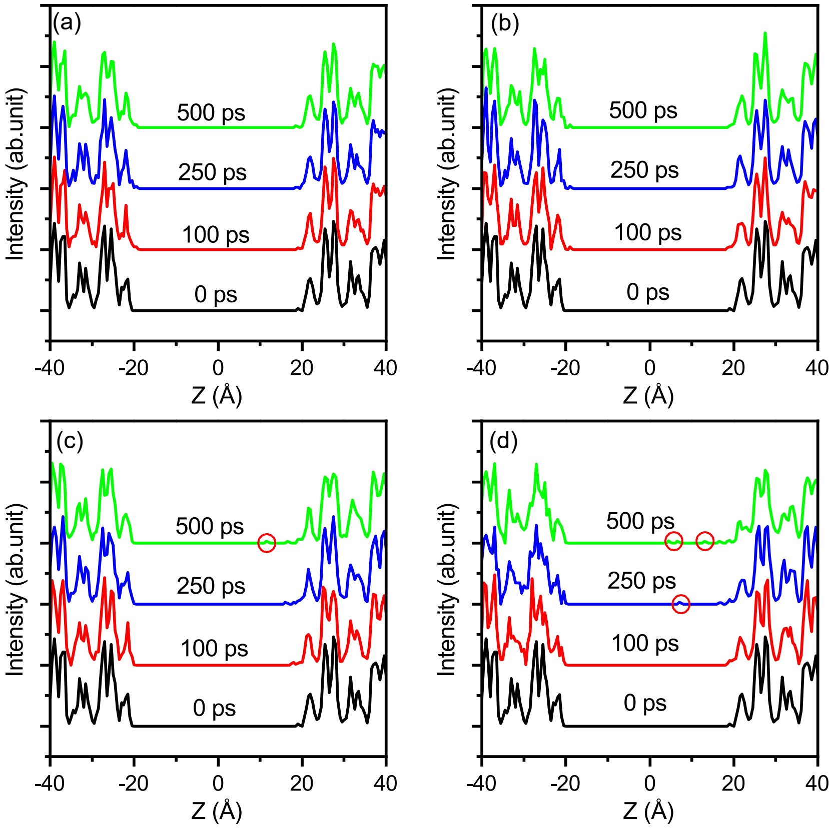

Fig. 9. Instantaneous distribution profiles of Ca^{2+} ions at different moments in the first 500 ps simulation at various temperatures. (a) 100 K, (b) 200 K, (c) 300 K and (d) 400 K.

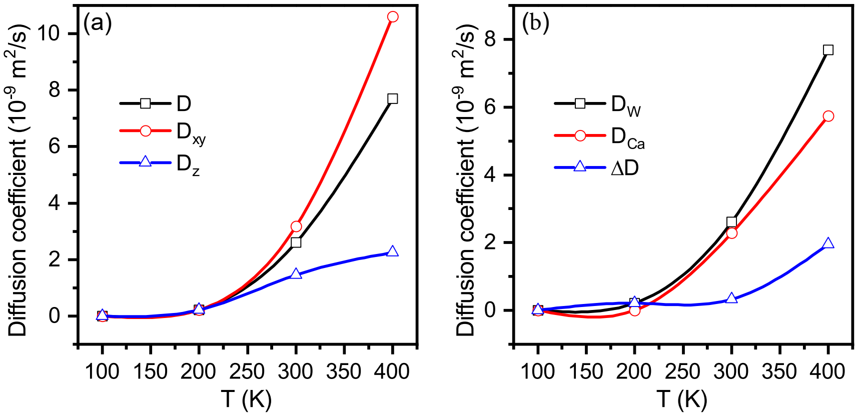

Fig. 10. (a) Relationship between overall diffusion coefficients of water molecules in nanopores and temperature, (b) comparison of overall diffusion coefficients of water molecules and Ca^{2+} ions in nanopores at various temperatures.

are distinct peaks on density profiles near C-S-H surfaces, corresponding to layered structures.

Because of the attractions from silica tetrahedral chains and Ca^{2+} ions, diffusion coefficients of water molecules near C-S-H surfaces are much smaller than those in the central regions of nanopores. Although values of overall diffusion coefficients of water molecules in nanopores increase with pore size, the anisotropy of diffusion coefficients still cannot be ignored, i.e., the diffusion coefficient along the direction parallel to C-S-H surfaces is larger than those perpendicular to C-S-H surfaces. As for Ca^{2+} ions, the ones on C-S-H surfaces move faster than those inside C-S-H substrates, and the corresponding diffusion coefficients are larger. Moreover, some Ca^{2+} ions desorb from C-S-H surfaces into nanopores, and the diffusion coefficients of these Ca^{2+} ions also increase with pore size. But the values of diffusion coefficients of these desorbed Ca^{2+} ions are smaller than those of water molecules, because water molecules would gather around Ca^{2+} ions and form clusters, hindering the movement of Ca^{2+} ions.

The structure and density distribution of water molecules in

C-S-H nanopores vary significantly with temperatures. When temperature is as low as 100 K, there are visible fluctuations on density profiles, and no layered structure is observed. As temperature increases, layered structures gradually form on C-S-H surfaces. However, it should be noticed that excessive temperature hinders the formation of layered structures of water molecules. As for dynamic properties, both the diffusion coefficients of water molecules and Ca^{2+} ions increase with temperature significantly. The anisotropy of the diffusion coefficients of water molecules and the difference between diffusion coefficient of water and Ca^{2+} ions are also much more pronounced in the cases with higher temperatures.

In conclusion, in this work, the structural and dynamic properties of water molecules and Ca^{2+} ions in C-S-H nanopores in scenarios with various pore sizes and temperatures are identified and compared. The results and findings would be useful in further understanding the transport behaviors of liquid water (such as capillary imbibition) in C-S-H nanopores and improving the mechanical properties and durability of cement-based materials.

Acknowledgements

The numerical calculations in this paper have been done on the supercomputing system in the Supercomputing Center of Wuhan University.

Conflict of interest

The authors declare no competing interest.

References

A, H., Yang, Z., Hu, R., et al. Molecular origin of wetting characteristics on mineral surfaces. Langmuir, 2023, 39(8): 2932-2942.

Alderete, N., Villagrán Zaccardi, Y., Snoeck, D., et al. Capillary imbibition in mortars with natural pozzolan, limestone powder and slag evaluated through neutron radiography, electrical conductivity, and gravimetric analysis. Cement and Concrete Research, 2019, 118: 57-68.

Bordallo, H. N., Aldridge, L. P., Desmedt, A. Water dynamics in hardened ordinary portland cement paste or concrete: From quasielastic neutron scattering. Journal of Physical Chemistry B, 2006, 110(36): 17966-17976.

Cao, Q., Xu, Y., Fang, J., et al. Influence of pore size and fatigue loading on NaCl transport properties in C-S-H nanopores: A molecular dynamics simulation. Materials, 2020, 13(3): 700.

Cerveny, S., Arrese-Igor, S., Dolado, J. S., et al. Effect of hydration on the dielectric properties of C-S-H gel. Journal of Chemical Physics, 2011, 134(3): 034509.

Cui, F., Jin, X., Liu, H., et al. Molecular modeling on gulong shale oil and wettability of reservoir matrix. Capillarity, 2022, 5(4): 65-74.

Cygan, R. T., Liang, J.-J., Kalinichev, A. G. Molecular models of hydroxide, oxyhydroxide, and clay phases and the development of a general force field. Journal of Physical Chemistry B, 2004, 108(4): 1255-1266.

Da, B., Yu, H., Ma, H., et al. Chloride diffusion study of coral concrete in a marine environment. Construction and Building Materials, 2016, 123: 47-58.

Dolado, J. S., Griebel, M., Hamaekers, J. A molecular dynamic study of cementitious calcium silicate hydrate (C-S-H) gels. Journal of the American Ceramic Society, 2007, 90(12): 3938-3942.

Greener, J., Peemoeller, H., Choi, C., et al. Monitoring of hydration of white cement paste with proton nmr spin-spin relaxation. Journal of the American Ceramic Society, 2004, 83(3): 623-627.

Hall, C. Capillary imbibition in cement-based materials with time-dependent permeability. Cement and Concrete Research, 2019, 124: 105835.

Heinz, O., Heinz, H. Cement interfaces: Current understanding, challenges, and opportunities. Langmuir, 2021, 37(21): 6347-6356.

Hou, D., Li, Z. Molecular dynamics study of water and ions transport in nano-pore of layered structure: A case study of tobermorite. Microporous and Mesoporous Materials, 2014a, 195: 9-20.

Hou, D., Li, Z. Molecular dynamics study of water and ions transported during the nanopore calcium silicate phase: Case study of jennite. Journal of Materials in Civil Engineering, 2014b, 26(5): 930-940.

Hou, D., Li, Z., Zhao, T., et al. Water transport in the nanopore of the calcium silicate phase: Reactivity, structure and dynamics. Physical Chemistry Chemical Physics, 2015, 17(2): 1411-1423.

Hou, D., Lu, Z., Li, X., et al. Reactive molecular dynamics and experimental study of graphene-cement composites: Structure, dynamics and reinforcement mechanisms. Carbon, 2017, 115: 188-208.

Hou, D., Zheng, H., Wang, P., et al. Molecular insight in the wetting behavior of nanoscale water droplet on CSH surface: Effects of Ca/Si ratio. Applied Surface Science, 2022, 587: 152811.

Ioannidou, K., Krakowiak, K. J., Bauchy, M., et al. Mesoscale texture of cement hydrates. Proceedings of the National Academy of Sciences of the United States of America, 2016, 113(8): 2029-2034.

Ioannidou, K., Labbez, C., Masoero, E. A review of coarse grained and mesoscale simulations of C-S-H. Cement and Concrete Research, 2022, 159: 106857.

Kai, M. -F., Hou, D. -S., Sanchez, F., et al. Nanoscale insights into the influence of seawater (NaCl) on the behavior of calcium silicate hydrate. Journal of Physical Chemistry C, 2023, 127(18): 8735-8750.

Kai, M. F., Zhang, L. W., Liew, K. M. New insights into creep characteristics of calcium silicate hydrates at molecular level. Cement and Concrete Research, 2021, 142: 106366.

Khan, M. N. A., Malik, A. H., Yaqub, M., et al. Development of high-temperature heavy density dolerite concrete for 4th generation nuclear power plants. Frontiers in Materials, 2023, 10: 1057637.

Korb, J. P., McDonald, P. J., Monteilhet, L., et al. Comparison of proton field-cycling relaxometry and molecular dynamics simulations for proton-water surface dynamics in cement-based materials. Cement and Concrete Research, 2007, 37(3): 348-350.

Kuusela, P., Pour-Ghaz, M., Pini, R., et al. Imaging of reactive transport in fractured cement-based materials with X-ray CT. Cement and Concrete Composites, 2021, 124(3): 104211.

Lange, D. A., Jennings, H. M., Shah, S. P. Image analysis techniques for characterization of pore structure of cement-based materials. Cement and Concrete Research, 1994, 24(5): 841-853.

Li, D., Zhao, W., Hou, D., et al. Molecular dynamics study on the chemical bound, physical adsorbed and ultra-confined water molecules in the nano-pore of calcium silicate hydrate. Construction and Building Materials, 2017, 151: 563-574.

Liu, J., Zhang, T., Sun, S. Stability analysis of the water bridge in organic shale nanopores: A molecular dynamic study. Capillarity, 2022, 5(4): 75-82.

Pellenq, R. J.-M., Kushima, A., Shahsavari, R., et al. A realistic molecular model of cement hydrates. Proceedings of the National Academy of Sciences of the United States of America, 2009, 106(38): 16102-16107.

Peterson, V. K., Brown, C. M., Livingston, R. A. Quasielastic and inelastic neutron scattering study of the hydration of monoclinic and triclinic tricalcium silicate. Chemical Physics, 2006, 326(2-3): 381-389.

Plimpton, S. Fast parallel algorithms for short-range molecular dynamics. Journal of Computational Physics, 1995, 117(1): 1-19.

Rakiewicz, E. F., Benesi, A. J., Grutzeck, M. W., et al. Determination of the state of water in hydrated cement phases using deuterium nmr spectroscopy. Journal of the American Chemical Society, 1998, 120(25): 6415-6416.

Scrivener, K., Ouzia, A., Juilland, P., et al. Advances in understanding cement hydration mechanisms. Cement and Concrete Research, 2019, 124: 105823.

Stepanova, N. A., The world's lowest temperature record. Weatherwise, 1963, 16(6): 268-269.

Tang, S. W., A, H. B., Chen, J. T., et al. The interactions between water molecules and C-S-H surfaces in loads-induced nanopores: A molecular dynamics study. Applied Surface Science, 2019, 496: 143744.

Wang, P. S., Ferguson, M. M., Eng, G., et al. ^{1}H nuclear magnetic resonance characterization of portland cement: Molecular diffusion of water studied by spin relaxation and relaxation time-weighted imaging. Journal of Materials Science, 1998, 33(12): 3065-3071.

Wang, F., Zhang, Y., Jiang, J., et al. Effect of temperature on the capillary transport of sodium sulfate solution in calcium silicate hydrate nanopore: A molecular dynamics study. Construction and Building Materials, 2020, 231: 117111.

Wróblewska, J., Kowalski, R. Assessing concrete strength in fire-damaged structures. Construction and Building Materials, 2020, 254: 119122.

Yang, L., Zhang, Y., Liu, Z., et al. In-situ tracking of water transport in cement paste using X-ray computed tomography combined with CsCl enhancing. Materials Letters, 2015, 160: 381-383.